

Rectangular Pixels for Efficient Color Image Sampling

Tripurari Singh^a and Mritunjay Singh^b

^aImage Algorithmics, 521 5th Ave W, #1003, Seattle, WA, USA 98119

^bImage Algorithmics, 147 Esplanade, Irvine, CA, USA 92612

ABSTRACT

We present CFA designs that faithfully capture images with specified luminance and chrominance bandwidths. Previous academic research has mostly been concerned with maximizing PSNR of reconstructed images without specific regard to chrominance bandwidth and cross-talk. Commercial systems, on the other hand, pay close attention to both these parameters as well as to the visual quality of reconstructed images. They commonly sacrifice resolution by using a sufficiently aggressive OLPF to achieve low cross-talk and artifact free images.

In this paper, we present the so called Chrominance Bandwidth Ratio, r , model in an attempt to capture both the chrominance bandwidth and the cross-talk between the various signals. Next, we examine the effect of tuning photosite aspect ratio, a hitherto neglected design parameter, and show the benefit of setting it at a different value than the pixel aspect ratio of the display. We derive panchromatic CFA patterns and corresponding photosite aspect ratios that provably minimize the photosite count for all values of r .

An interesting outcome is a CFA design that captures full chrominance bandwidth, yet uses fewer photosites than the venerable color-stripe design. Another interesting outcome is a low cost practical CFA design that captures chrominance at half the resolution of luminance using only 4 unique filter colors, that lends itself to efficient linear demosaicking, and yet vastly outperforms the Bayer CFA with identical number of photosites demosaicked with state of the art compute-intensive nonlinear algorithms.

Keywords: CFA, Demosaicking, Color, Filter, Photosite, Pixel, Aspect Ratio

1. INTRODUCTION

A popular design for capturing color images with a single image sensor is to overlay it with a Color Filter Array (CFA). An old and effective design is the color-stripe sensor that tiles red, green and blue filters in alternating vertical or horizontal stripes. This design yields red, green and blue images of equal resolution, or equivalently, luminance and chrominance signals of equal bandwidth. The color-stripe design is still used in high end cameras.¹ Newer CFA designs by Bayer² and others,³⁻⁸ make different trade-offs between luminance and chrominance bandwidths as well as the crosstalk between them.

Most of the early CFAs as well as their associated demosaicking algorithms were empirically designed. A significant breakthrough was made by^{9,10} who analyzed electromagnetic filtering performed by CFAs as amplitude modulation of color components in the spatial domain. This led to elegant frequency domain demosaicking techniques that viewed the problem as that of demultiplexing the luminance and chrominance signals via demodulation and filtering.⁹⁻¹⁴

The complementary problem of designing CFAs with good frequency domain properties was first attacked by¹⁰ wherein the doubling of the number of blue photosites in the Bayer CFA was suggested. This was followed by techniques to design CFAs directly in the frequency domain by³⁻⁵ and optimized by.^{7,8} These techniques fix the pattern of each primary color to consist of a small set of spatial “carriers” - two dimensional sinusoids with appropriate frequencies, phases and amplitudes - and sum over the three primaries to arrive at the final pattern. This pattern is then printed over the sensor. When an image formed by the camera’s lens is filtered by the CFA,

Further author information: (Send correspondence to T.S.)

T.S.: E-mail: tsingh@imagealgorithmics.com, Telephone: 1 503 333 4902

M.S.: E-mail: msingh@imagealgorithmics.com, Telephone: 1 503 382 7960

Patent pending

it is modulated by each of the carrier frequencies. The overlap of the modulation sidebands of the 3 primaries induces a color transform and leads to a multiplex of luminance and chrominance signals modulated at different frequencies. As long as there is limited cross-talk between the luminance and chrominance signals, and the color transform is invertible the original color image can be recovered.^{9,10,12}

It is important to note the role of the CFA in determining the noise figure of the camera. The relative quantum efficiency of each photosite should be approximately uniform to control sensor saturation. Furthermore, the color transform should have a numerically stable inverse and the transmission of light through the CFA should be maximized. It is interesting to note that the latter two are often conflicting objectives and the trade-off depends on the application for which the camera is designed. A low light camera might benefit from high transmittivity⁷ while a studio camera - where lighting can be controlled - would do better with a numerically stable color inverse.

Another factor influencing the choice of color transform is the high frequency content of chrominance signals. Well chosen color transforms result in chrominance signals with low high frequency content. This allows the chrominance signals to be placed close to each other and to the luminance signal without significant cross-talk.^{2-8,15}

Perhaps the most important factor influencing the close packing of luminance and chrominance signals is the geometry of their spectra. Square/rectangular sampling lattices admit higher resolution along the diagonal directions than along horizontal or vertical. Optical systems, on the other hand, generate roughly equal resolution in all directions thereby yielding images with nearly circular spectral support. This leads to the problem of efficiently packing circles into squares/rectangles. *Tackling this packing problem is the main focus of this paper.*

An aggressive technique for close packing of luminance and chrominance employs adaptive directional techniques during demosaicking.^{11-13,16-23} These techniques assume the luminance and chrominance spectra of small image patches to have low bandwidth in at least one direction. They design their CFA to generate more than one copy of chrominance spectrum/spectra, identify the cleanest copy during the demosaicking step and use directional filtering to demultiplex them. The benefits of adaptive directional demosaicking come at a heavy cost, though, since sensing edge directions from noisy subsampled images is a hard problem and the non-linear nature of decision making makes noise reduction a non-separable step. To avoid these complications, CFA designs presented in this paper do not need adaptive demosaicking.

2. AMPLITUDE MODULATION IN THE DISCRETE DOMAIN

Modulating a two dimensional signal with a carrier of frequency $\boldsymbol{\omega} = (\omega_1, \omega_2)$, $-\pi < \omega_1, \omega_2 < \pi$ yields a shifted spectral copy of the signal - known as a sideband - centered about $\boldsymbol{\omega}$. A real carrier composed of a conjugate pair of sinusoids of frequencies $(-\omega_1, -\omega_2), (\omega_1, \omega_2)$ - $-\pi < \omega_1, \omega_2 < \pi$ generates two shifted spectral copies of the baseband.

In the special case of a real carrier composed of the conjugate sinusoid pair $(\pm\pi, 0)$, the aliases collapse to the same sinusoid pair. Since sideband frequencies $\leq -\pi$ and $\geq \pi$ are aliased this results in just one spectral copy of the baseband. The case of $(0, \pm\pi)$ is symmetrical.

Another special case arises with the real carrier composed of a conjugate sinusoid pair $(-\pi, -\pi), (\pi, \pi)$. Along with its aliases, this carrier occupies the four corner frequencies $(\pm\pi, \pm\pi)$. Since only a quarter of a spectral copy of the baseband signal survives aliasing at each corner, a total of just one spectral copy is preserved.

Frequencies are a precious resource in CFAs and attempts are made to avoid duplicating spectral copies. A natural strategy is to use the carrier frequencies that result in a single spectral copy,²⁻⁶ as mentioned above. An alternate strategy is to use carrier frequencies that generate two sidebands but multiplex two signals by varying the phase of the carrier for each. Quadrature modulation^{7,8} is one such technique wherein the phase difference between the carriers is set to $\frac{\pi}{2}$.

3. CFA DESIGN PRELIMINARIES

Consider a photosite located at $\mathbf{n} = (n_1, n_2)$ that filters incident light $\mathbf{x}(\mathbf{n}) = [x_r(\mathbf{n}) \ x_g(\mathbf{n}) \ x_b(\mathbf{n})]^T$ through color filter array $\mathbf{c}(\mathbf{n}) = [c_r(\mathbf{n}) \ c_g(\mathbf{n}) \ c_b(\mathbf{n})]$ and measures the resulting noise-free, scalar signal $y(\mathbf{n})$, where

$$y(\mathbf{n}) = \mathbf{c}(\mathbf{n}) \cdot \mathbf{x}(\mathbf{n}) \quad (1)$$

Consider a set of *real* carrier sinusoids $s^{(k)}(\mathbf{n})$, $1 \leq k \leq m$ of unit amplitude, frequencies $\boldsymbol{\omega}^{(k)} = (\omega_1^{(k)}, \omega_2^{(k)})$ and phases $\phi^{(k)} \in \{0, \frac{\pi}{2}\}$, given by

$$s^{(k)}(\mathbf{n}) = \frac{e^{j(\boldsymbol{\omega}^{(k)} \cdot \mathbf{n} + \phi^{(k)})} + e^{-j(\boldsymbol{\omega}^{(k)} \cdot \mathbf{n} + \phi^{(k)})}}{2} \quad (2)$$

Each color of the panchromatic CFA, $c_i(\mathbf{n})$, $i \in \{r, g, b\}$, is the superposition of these carriers scaled by an appropriate real amplitude $a_i^{(k)}$,

$$c_i(\mathbf{n}) = \sum_{k=1}^m a_i^{(k)} s^{(k)}(\mathbf{n}) \quad (3)$$

The choice of carrier frequencies is a CFA design decision except for the DC component, whose presence is essential for physically realizable CFAs. For this reason we set $\boldsymbol{\omega}^{(1)} = (0, 0)$. It follows that $a_i^{(1)} > 0$, $i \in \{r, g, b\}$.

Once the sensor is exposed to image $\mathbf{x}(\mathbf{n})$ and its mosaiced output $\mathbf{y}(\mathbf{n})$ is captured, a demosaicking step is needed to reconstruct $\mathbf{x}(\mathbf{n})$. Assuming the carrier frequencies $\boldsymbol{\omega}^{(k)}$, $1 \leq k \leq m$ are sufficiently separated so that sidebands centered about them do not overlap, each modulated signal can be recovered by multiplication with its respective carrier followed by convolution with a low pass filter $h^{(k)}$. Formally,

$$u^{(k)}(\mathbf{n}) = (h^{(k)} * (s^{(k)} \cdot \mathbf{y}))(\mathbf{n}) \quad (4)$$

Each $u^{(k)}(\mathbf{n})$, $0 \leq k \leq m$ can be viewed as a color component. Motivated by the fact that $a_i^{(1)} > 0$, $i \in \{r, g, b\}$, we loosely refer to $u^{(1)}(\mathbf{n})$ as the luminance signal, and $u^{(k)}(\mathbf{n})$, $k > 1$ as the chrominance signals.

Since $\mathbf{u}(\mathbf{n}) = [u^{(1)}(\mathbf{n}) \ u^{(2)}(\mathbf{n}) \ \dots \ u^{(m)}(\mathbf{n})]^T$ is generated by the modulation of the incident image $\mathbf{x}(\mathbf{n})$, it can be written as

$$\mathbf{u}(\mathbf{n}) = \mathbf{A} \cdot \mathbf{x}(\mathbf{n}) \quad (5)$$

where $\mathbf{A} = \begin{bmatrix} a_r^{(1)} & a_g^{(1)} & a_b^{(1)} \\ a_r^{(2)} & a_g^{(2)} & a_b^{(2)} \\ \vdots & \vdots & \vdots \\ a_r^{(m)} & a_g^{(m)} & a_b^{(m)} \end{bmatrix}$. \mathbf{A} can be interpreted as the color transform matrix, and provided its rank is 3, \mathbf{x} can be recovered by

$$\mathbf{x}(\mathbf{n}) = \mathbf{A}^{-1} \cdot \mathbf{u}(\mathbf{n}) \quad (6)$$

Here \mathbf{A}^{-1} , the generalized inverse of \mathbf{A} , can be interpreted as the inverse color transform.

From the above discussion it is clear that the three decision variables for a CFA design are the carrier frequencies $\boldsymbol{\omega}^{(k)}$, $1 \leq k \leq m$, phases $\phi^{(k)}$, $1 \leq k \leq m$ and amplitudes given by the matrix \mathbf{A} .

4. CFA OPTIMIZATION

Equation 5 shows that the carrier amplitudes determine the color transform. A good choice of \mathbf{A} generates chrominance signals with minimal high frequency energy content¹⁵ thereby enabling a close packing of luminance and chrominance spectra.

The choice of \mathbf{A} also effects the sensitivity of the sensor and noise amplification in the demosaicking step. In particular, \mathbf{A} effects the transmittivity of the CFA and its variation as a function of \mathbf{n} which, in turn, determine the sensor's sensitivity and the unevenness of its exposure to desaturated colors respectively. $\|\mathbf{A}^{-1}\|$, on the other hand, determines noise amplification in the demosaicking step due to numerical instability. For detailed discussions of the trade-offs involved in selecting \mathbf{A} we direct the reader to.^{3-5, 7, 8, 15}

In section 3, we limited the choice of carrier phases, $\phi^{(k)}$, to the pair $\{0, \frac{\pi}{2}\}$. Arbitrary values of $\phi^{(k)}$ can be made to work, but the mathematics needs to be slightly modified. In particular, the color transform matrix \mathbf{A} gets altered with sensitivity and noise ramifications similar to those mentioned above. We leave the optimization of $\phi^{(k)}$, $1 \leq k \leq m$ as an open problem.

4.1 The Chrominance Bandwidth Ratio Model

In the rest of this paper we attack the problem of designing CFAs that use a minimum number of photosites by compactly packing their luminance and chrominance spectra. We define a parameter of the problem, the Chrominance Bandwidth Ratio, r , as the maximum ratio of chrominance and luminance bandwidths of the *input* image that a CFA can faithfully capture.

Now, only synthetic or processed images have lower chrominance bandwidth than luminance. As a result, natural images sensed by a CFA with $r < 1$ suffer from crosstalk, the magnitude of which is a function of the input image and has to be empirically determined. This makes it impossible to define a measure of CFA quality, for $r < 1$, that does not depend on the input image. However, since crosstalk monotonically vanishes with r , and in the vast majority of the images very rapidly so, the Chrominance Bandwidth Ratio, r , serves as a reasonable surrogate for image quality.

4.2 Photosite Aspect Ratio

An important but hitherto under-tuned CFA parameter is their photosite aspect ratio. Sensor photosites usually have the same aspect ratio as the display pixels their designers target, which are usually square. Important exceptions are legacy video standards that feature different horizontal and vertical resolutions resulting in rectangular pixels.

We study sensors with photosite aspect ratios that are different from the pixel aspect ratios of the displays they target. Color stripe CFAs already employ this design, fitting three photosites in the space of one along the direction orthogonal to their stripes.

To ease analysis and visualization of spectra from rectangular photosites, we introduce Pitch-Scaled Fourier Diagrams. PSFDs plot the (discrete) Fourier transform of a discrete signal on frequency axes that are scaled inversely as the photosite pitch along it so that a unit length along any direction represents the same continuous domain resolution. Thus, spectra of discretized isotropic optical images are plotted as circles and the Fourier support of the square CFA patch on which the image is incident is plotted as a rectangle with an aspect ratio that is the reciprocal of its photosite aspect ratio. The area of the rectangle is proportional to the number of photo sites contained in the CFA patch, so that the CFA photosite minimization problem is reduced to packing the circular spectra of luminance and chrominance into a rectangle of minimum area whose aspect ratio is of our choosing.

5. OPTIMUM PACKING OF SPECTRA

Consider a camera with an optical system that resolves spatial frequencies up to a maximum of ω^* radians/mm. In what follows we refer to the act of minimizing the number of photosites of a CFA as “optimization” and a CFA that faithfully captures an optical image of a given Chrominance Bandwidth Ratio, r , with the minimum number of photosites as an optimum CFA. Note that optimum CFAs are panchromatic, in general. They are also not unique, in general, since there is often more than one way of compactly packing the luminance and chrominance spectra.

To capture color images according to the Chrominance Bandwidth Ratio model, a CFA design with the minimum number of photosites has 4 cases as outlined in table 1. The PSFD of the input image modulated by the CFA for all four cases contain baseband luminance surrounded by one copy each of the two chrominance signals quadrature modulated by a carrier on the edge of the diagram. See figure 1. These 4 cases yield 2 types of PSFDs, one with its carrier on the long edge of the rectangle and the other on the short edge.

5.1 Proof of Optimality

We now prove that no CFA design, for a given Chrominance Bandwidth Ratio, r , has fewer photosites than that described in table 1. To ease our analysis, we switch to PSFDs with frequency range from 0 to 2π along both the x and the y axes. Note that figure 1 and table 1 use the more popular $-\pi$ to π range.

We start our proof with a lemma on the location of luminance in the PSFD.

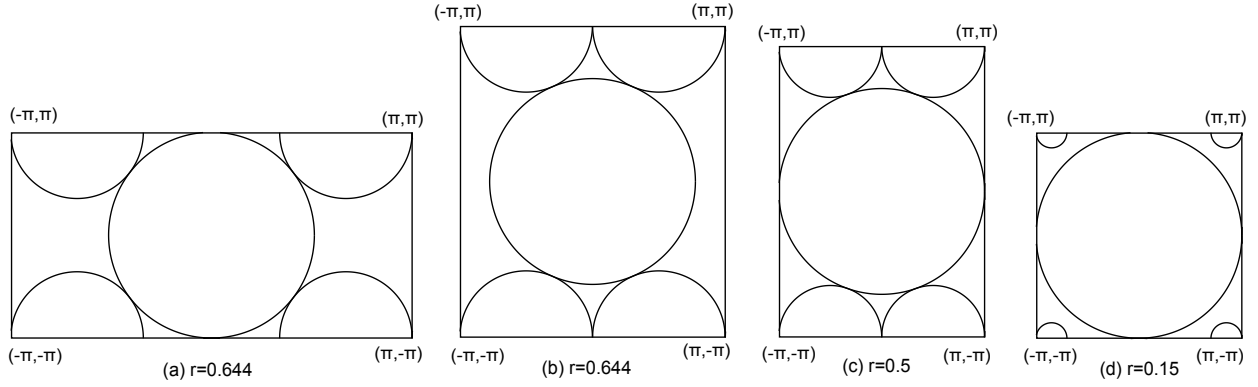


Figure 1. PSFDs of optimum CFAs

r	$\omega^{(2)}$ (rad/sample)	d_x (mm)	d_y (mm)	Aspect Ratio
[0,0.25]	$(\pm(1-r)\pi, \pm\pi)$	$\frac{\pi}{\omega^*}$	$\frac{\pi}{\omega^*}$	1:1
[0.25,0.5]	$(\pm(1-r)\pi, \pm\pi)$	$\frac{\pi}{\omega^*}$	$\frac{\pi}{2\sqrt{r}\omega^*}$	$\frac{1}{2\sqrt{r}} : 1$
[0.5,0.644]	$(\pm\frac{\pi}{2}, \pm\pi)$	$\frac{\pi}{2r\omega^*}$	$\frac{\pi}{\sqrt{(2r+1)\omega^*}}$	$\frac{2r}{\sqrt{2r+1}} : 1$
[0.644,1]	$(\pm\frac{\sqrt{(1+r)^2-1}}{\sqrt{(1+r)^2-1+r}}\pi, \pm\pi)$	$\frac{\pi}{(\sqrt{(1+r)^2-1+r}\omega^*)}$	$\frac{\pi}{\omega^*}$	$\sqrt{(1+r)^2-1} + r : 1$

Table 1. Optimum solution as a function of r . d_x and d_y here are defined as the photosite pitch in the x and y directions respectively.

LEMMA 1. All physically realizable CFAs modulate their luminance signal about $(0, 0)$, $(2\pi, 0)$, $(2\pi, 2\pi)$ and $(0, 2\pi)$.

Proof. All filters in a physically realizable CFA are non-negative. Furthermore, since non trivial CFAs admit some light of each primary color, the Fourier transform of each primary color has a positive DC component. This, in turn, admits the luminance of the input image as a baseband which is distributed about the 4 aliases of DC, i.e. $\omega^{(1)} = (0, 0) = (2\pi, 0) = (2\pi, 2\pi) = (0, 2\pi)$. \square

Transforming the results of section 2 to PSFDs ranging from $[0, 2\pi]$ along x and y axes we find 3 real carrier frequencies that generate a single sideband, namely (π, π) , the aliased pair $(\pi, 0)$, $(\pi, 2\pi)$ and the aliased pair $(0, \pi)$, $(2\pi, \pi)$. All other real carriers generate two sidebands.

In the next lemma we optimize CFAs that quadrature modulate the two chrominance signals with a real carrier that generates two sidebands. We postpone discussion of the single sideband carrier case to theorem 1.

LEMMA 2. A CFA that faithfully captures color images with Chrominance Bandwidth Ratio $r \in [0, 1]$, and is constrained to do so by quadrature modulating both chrominance signals with one real carrier frequency that generates two sidebands, has minimal number of photosites if it is designed as per table 2.

r	$\omega^{(2)}$ (radians/sample)	d_x (mm)	d_y (mm)
[0,0.25]	$((1-r)\pi, \pi), ((1+r)\pi, \pi)$	$\frac{\pi}{\omega^*}$	$\frac{\pi}{\omega^*}$
[0.25,0.5]	$((1-r)\pi, \pi), ((1+r)\pi, \pi)$	$\frac{\pi}{\omega^*}$	$\frac{\pi}{2\sqrt{r}\omega^*}$
[0.5,0.644]	$(\frac{\pi}{2}, \pi), (\frac{3\pi}{2}, \pi)$	$\frac{\pi}{2r\omega^*}$	$\frac{\pi}{\sqrt{(2r+1)\omega^*}}$
[0.644,1]	$(\frac{\sqrt{(1+r)^2-1}}{\sqrt{(1+r)^2-1+r}}\pi, \pi), (\frac{\sqrt{(1+r)^2-1+2r}}{\sqrt{(1+r)^2-1+r}}\pi, \pi)$	$\frac{\pi}{(\sqrt{(1+r)^2-1+r}\omega^*)}$	$\frac{\pi}{\omega^*}$

Table 2. Table for lemma 2. r , d_x and d_y are defined as the Chrominance Bandwidth Ratio, photosite pitch in the x and y directions respectively.

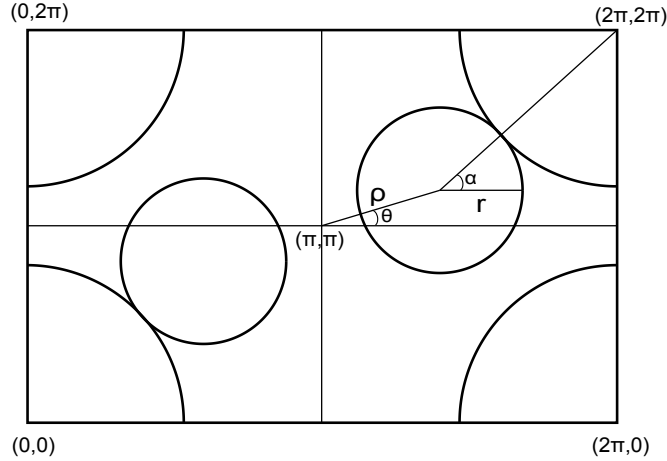


Figure 2. PSFD with range $[0, 2\pi]$ along both axes for lemma 2

Proof.

We use the polar representation (ρ, θ) to denote the conjugate carrier frequency pair $((1 - \rho \cos \theta)\pi, (1 - \rho \sin \theta)\pi)$, $((1 + \rho \cos \theta)\pi, (1 + \rho \sin \theta)\pi)$ as shown in figure 2. We note that $\rho \geq r$ to prevent chrominance sidebands from overlapping and limit $0 \leq \theta \leq \frac{\pi}{2}$ as the remaining values of θ are symmetrical. Furthermore, we denote by α the angle between the x-axis and the line joining the carrier $((1 + \rho \cos \theta)\pi, (1 + \rho \sin \theta)\pi)$ with $(2\pi, 2\pi)$.

Simple trigonometry gives the height of the PSFD of a unit square patch of the CFA as $c \cdot \max(1, \rho \sin \theta + \max(r, (1 + r) \sin \alpha))$ where c is a scaling constant used to plot the PSFD. Similarly the width of the PSFD is $c \cdot \max(1, \rho \cos \theta + \max(r, (1 + r) \cos \alpha))$ and the area of the PSFD is the product height and width. This area is minimized by setting $\rho = r$, $\theta = 0$ for all r , and setting α so as to minimize the width of the PSFD, or its height, or both, depending on r as described below.

1. $0 \leq r \leq 0.25$: In this case α is chosen so as to minimize both the width and the height of the PSFD. Pixel pitches do not have to be made finer to capture color, and can be set to the Nyquist rate of luminance.
2. $0.25 < r \leq 0.5$: In this case α is chosen to minimize the width of the PSFD but not its height. Pixel pitch is made finer than the Nyquist rate of luminance in the vertical direction to accommodate the chrominance sidebands.
3. $0.5 < r \leq 0.644$: As in the previous case α is chosen to minimize the width of the PSFD but not its height. However pixel pitch is made finer than the Nyquist rate of luminance along both vertical and horizontal directions to accommodate the chrominance sidebands.
4. $0.644 \leq r \leq 1$: In this case α is chosen to minimize the height of the PSFD. Pixel pitch is made finer than the Nyquist rate of luminance in the horizontal direction to accommodate the chrominance sidebands.

Applying elementary Euclidean geometry to the above cases we get the results of table 2. \square

We now present the final piece of our proof.

THEOREM 1. *Given an optical image with luminance bandlimited to $[0, \omega^*]$ radians/mm and chrominance bandlimited to $[0, r\omega^*]$ radians/mm, a CFA with photosite pitch and carrier frequencies specified by table 1 has the lowest photosite count of all CFAs that can pack the luminance and chrominance spectra without overlap.*

Proof. Lemma 2 describes CFAs that use one real carrier with two sidebands to quadrature modulate its two chrominance signals. Clearly any CFA that employs additional carriers - with one or two sidebands - can do no better.

This leaves CFAs that employ carriers with only one sideband. There are 3 such carriers, namely (π, π) , the aliased pair $(\pi, 0)$, $(\pi, 2\pi)$ and the aliased pair $(0, \pi)$, $(2\pi, \pi)$. We need only consider CFA designs that use 2 carriers since adding the third cannot lower photosite count. There are 3 ways to select 2 carriers of which 2 are symmetrical leaving 2 CFA designs to consider. Both these CFAs use the the aliased pair $(\pi, 0)$, $(\pi, 2\pi)$ as one carrier and use either (π, π) , or the aliased pair $(0, \pi)$, $(2\pi, \pi)$ as the other. These 2 CFA designs can be easily analyzed and shown to perform worse than the two sideband solution of lemma 2, for all values of r .

Transforming the results of lemma 2 from 0 to 2π frequency range to $-\pi$ to π frequency range, we get the results of table 1. \square

5.2 Demosaicking

Demosaicking is accomplished by the standard technique of frequency domain demultiplexing.^{9,10,12} Specifically, chrominance image components are recovered by multiplication with their respective carriers followed by low pass filtering. The baseband luminance signal can be extracted by one of two standard techniques: low pass filtering of the mosaiced image or subtracting out re-modulated copies of the two chrominance signals from the mosaiced image.

All filters can be implemented with separable designs with minor loss of performance. Conversion between photosite and the storage/display pixel aspect ratios can also be built into these separable filters, as can post-demosaick sharpening.

Finally the inverse color transform is applied, which can itself be combined with color transformation for color correction and compression. The resulting algorithm is very efficient and can be implemented in compact video cameras.

5.3 Periodicity of the Optimum CFA

Not all optimum CFAs outlined in section 5 have patterns with small periods, if they are periodic at all. Manufacturing such a CFA requires a large number of unique filter colors.

The number of unique colors required can be reduced by approximating the optimum CFAs by CFAs with small periods, as outlined in table 3. This table provides pixel pitches once a rational approximation $\frac{\alpha}{\beta}$ of $\frac{\omega_1^{(2)}}{\pi}$ is determined. Separate formulas for both $\frac{\alpha}{\beta} > \frac{\omega_1^{(2)}}{\pi}$ and $\frac{\alpha}{\beta} < \frac{\omega_1^{(2)}}{\pi}$ are given.

r	$\frac{\alpha}{\beta} > \frac{\omega_1^{(2)}}{\pi}$	d_x (mm)	d_y (mm)	Aspect Ratio
[0.25,0.5]	Yes	$\frac{(\beta-\alpha)\pi}{r\beta\omega^*}$	$\frac{\pi}{2\sqrt{r}\omega^*}$	$\frac{r\beta}{2\sqrt{r}(\beta-\alpha)} : 1$
[0.25,0.5]	No	$\frac{\pi}{\omega^*}$	$\frac{\pi}{\sqrt{(1+r)^2 - (\frac{\alpha}{\beta})^2}\omega^*}$	$\frac{1}{\sqrt{(1+r)^2 - (\frac{\alpha}{\beta})^2}} : 1$
[0.5,0.644]	Pattern is periodic with a period of 2x4 pixels and 4 unique colors			
[0.644,1]	Yes	$\frac{(\beta-\alpha)\pi}{r\beta\omega^*}$	$\frac{\pi}{\omega^*}$	$\frac{r\beta}{(\beta-\alpha)} : 1$
[0.644,1]	No	$\frac{\alpha\pi}{\beta\sqrt{(1+r)^2 - 1}\omega^*}$	$\frac{\pi}{\omega^*}$	$\frac{\beta\sqrt{(1+r)^2 - 1}}{\alpha} : 1$

Table 3. Pitch modifications for CFA pattern periodicity

5.4 Color Overhead

Depending on the Chrominance Bandwidth Ratio, CFAs need more photosites to capture an unit square image patch than a (monochrome) sensor operating at the Nyquist rate does. We refer to this extra photosite count, expressed as a proportion of the photosite count for a Nyquist rate sensor, as the *color overhead*. Formally, color overhead = $\frac{\pi^2}{\omega^{*2} \cdot d_x \cdot d_y} - 1$.

Color overheads of the proposed CFA along with a few popular designs *using demodulate and filter demosaicking of section 5.2* are plotted in figure 3. Note that state of the art nonlinear demosaicking of Bayer yields much better results than that plotted in figure 3. A comprehensive comparison of the state of the art Bayer CFA demosaicking with the proposed optimum CFA is undertaken in section 8.

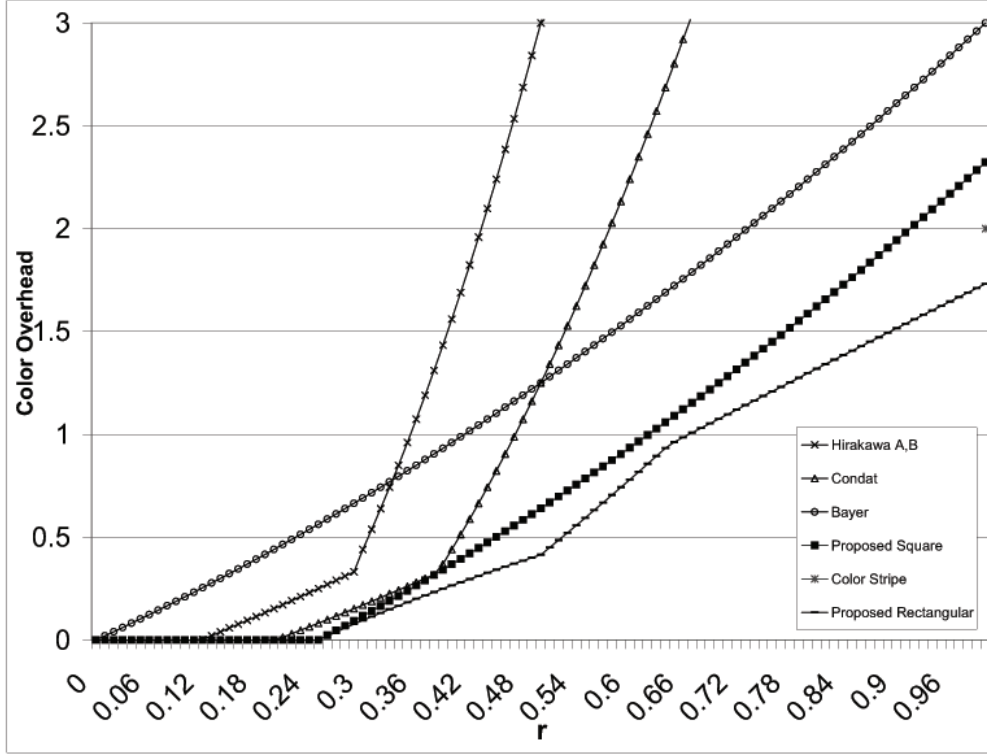


Figure 3. Color Overhead of various CFAs when demosaicked with non-adaptive demodulate & filter algorithms for extraction of chrominance.

6. OPTIMUM PACKING WITH SQUARE PHOTOSITES

An optimization exercise similar to section 5 can be carried out with square photosites with slightly poorer results. The results are outlined in table 4 and color overheads are plotted in figure 3. It is important to note that the periodicities of the optimum square photosite CFAs are different from those of the optimum rectangular photosite CFAs of section 5.

r	$d_x=d_y$ (mm)	$\omega^{(2)}$ (rad/sample)
$[0,0.25]$	$\frac{\pi}{\omega^*}$	$(1-r)\pi$
$[0.25,0.809]$	$\frac{2\pi}{(r+\sqrt{r^2+4r+2})\omega^*}$	$\frac{-r+\sqrt{r^2+4r+2}}{r+\sqrt{r^2+4r+2}}\pi$
$[0.809,1]$	$\frac{\pi}{2r\omega^*}$	$\frac{\pi}{2}$

Table 4. Optimum square-pixel CFA design as a function of r

7. OPTIMUM CFA FOR CHROMINANCE BANDWIDTH RATIO = 1

In this section we compare the venerable color stripe CFA with the optimally packed CFA of section 5 with $r = 1$. The PSFD of the optimum CFA is similar to figure 1(a), while that of the color stripe CFA has chrominance at $(-\frac{2\pi}{3})$ and $(\frac{2\pi}{3})$ and luminance at $(0, 0)$.

The pixel pitches of the color stripe CFA are $d_x = \frac{\pi}{\omega^*}$ and $d_y = \frac{\pi}{3\omega^*}$. The pixel pitches of the optimum CFA, on the other hand, are $d_x = \frac{\pi}{\omega^*}$ and $d_y = \frac{\pi}{(1+\sqrt{3})\omega^*} = \frac{2.73\pi}{\omega^*}$. Thus the optimum CFA needs 9% fewer photosites than the color stripe CFA to capture the same luminance and chrominance resolution.

The chrominance carrier frequency of the optimum CFA and its aliases are $\omega^{(2)} = (\pm\pi, \pm\frac{\sqrt{3}}{\sqrt{3+1}}\pi)$. $\omega^{(2)}$ is irrational and hence this CFA pattern is aperiodic with each filter having a unique color. A rational approximation

of the optimum CFA can be devised in accordance with section 5.3, which trades off the number of photosites with the number of unique CFA colors.

While the CFA presented in this section is of obvious theoretical interest, its practicality depends on the relative difficulties in manufacturing CFAs with larger numbers of photosites vs the difficulties in manufacturing sensors with larger number of unique color filters as well as the computational cost of demosaicking.

8. OPTIMUM CFA FOR CHROMINANCE BANDWIDTH RATIO = 0.5

Perhaps the most practical result of this paper is the optimum CFA design for $r = 0.5$. This design is interesting for a number of reasons. Firstly, $r = 0.5$ yields chrominance bandwidth that is half that of luminance, which is a popular consumer still and video standard. Secondly, crosstalk is practically imperceptible on most natural images if a good color space is chosen, such as Hel-Or's.¹⁵ Thirdly, the CFA has a small 4x2 repeating pattern with only 4 unique colors. Fourthly, this CFA captures roughly the same luminance and chrominance resolution with linear demodulate and filter demosaicking as the Bayer CFA does with the state of the art non-linear demosaicking, and does so with substantially reduced artifacts and higher PSNR. Fifthly, this design generates cleaner images in the presence of sensor noise and, unlike non-linear demosaicking used for Bayer, allows noise reduction to be a separable step without loss of efficacy. Sixthly and lastly, linear demosaicking of this CFA can be implemented cheaply using separable filters thereby offering the prospect of very high quality images from compact still and video cameras.

PSFD of the optimum $r = 0.5$ CFA is shown in figure 1(c). Chrominance is quadrature modulated with a carrier and its aliases $\omega^{(2)} = (\pm\frac{\pi}{2}, \pm\pi)$. The photosite pitches of this CFA are $d_x = \frac{\pi}{\omega^*}$ and $d_y = \frac{\pi}{\sqrt{2}\cdot\omega^*}$ so that the photosite aspect ratio is $\sqrt{2} : 1$. This CFA has a 4x2 repeating pattern with only 4 unique colors. A concrete example of such a CFA is described in the experimental section 8.1 and shown in figure 4.

8.1 Experimental Results

We empirically compare the proposed CFA optimized for $r = 0.5$ with the Bayer CFA using a MATLAB simulation of the imaging pipeline. Most academic CFA research neglect the optical imaging pipeline and study the image after it has been discretized. In our setup we model the OLPF as a Gaussian Diffuser and also simulate the box filtering caused by non-zero pixel size. We start with an input image with resolution that is twice the Nyquist limit of the system so as to simulate aliasing caused by Optical Low Pass Filter (OLPF) leakage at high frequencies. We compensate for the effects of the optical pipeline by performing post-demosaick inverse filtering and sharpening with Adobe Photoshop's unsharp filter as is the standard practice in commercial systems. The demosaicked image is compared with the original image put through an imaging pipeline consisting of the same OLPF, box filtering, inverse box filtering and sharpening, but not the CFA.

We tested the Bayer CFA with the OLPF tuned to a color overhead of 20% so that it lets in frequencies upto 83% of the Nyquist frequency. This is roughly the color overhead of commercial systems. For demosaicking we selected Hirakawa & Parks' AHD¹⁸ algorithm since it is a practical algorithm with mild artifacts that has become the de-facto standard for open source raw converters. We also tested Gunturk et. al's POCS²⁴ and found it to perform marginally worse than AHD thereby confirming the popular choice of AHD under practical settings.

In the proposed CFA design, we use Hel-Or's Canonical Correlation Analysis¹⁵ derived color transform in order to minimize chrominance energy. The colors of this panchromatic CFA are given in figure 4. The photosites used by the Bayer CFA are square and same in number as the proposed CFA.

All experiments were performed on the Kodak image set with identical optical pipelines. Results are summarized in table 5. The proposed CFA shows a robust 7.6dB improvement in average PSNR over the AHD demosaicked Bayer CFA and 10.3dB over the POCS demosaicked Bayer CFA, and outperforms the two in every image.

The Kodak images are quite small to begin with and further downsized by a factor 2 by the optical pipeline simulation. For improved visibility we also ran our simulations on a large, high resolution image.

Without sensor noise, our experiments yield MSEs of 1.51, 11.3, 27.0 for the proposed CFA, AHD and POCS respectively. Next we add Gaussian noise with $\sigma = 0.8$, so that the noise is comparable in magnitude to the

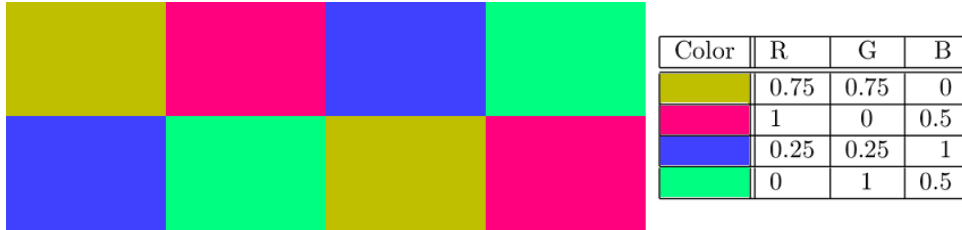


Figure 4. Optimum panchromatic CFA pattern for $r = 0.5$ used in section 8.

Image	Proposed	AHD	POCS	Image	Proposed	AHD	POCS
kodim01	45.0	39.3	35.6	kodim13	45.2	37.2	36.5
kodim02	44.2	37.7	34.2	kodim14	38.5	30.1	27.3
kodim03	44.8	37.1	32.4	kodim15	44.6	38.2	35.3
kodim04	45.0	37.4	34.5	kodim16	48.3	42.0	40.0
kodim05	41.8	32.2	29.8	kodim17	47.0	39.6	39.0
kodim06	46.1	39.6	37.3	kodim18	44.8	36.4	34.1
kodim07	44.0	35.3	33.1	kodim19	46.4	38.6	36.8
kodim08	43.7	35.3	32.8	kodim20	46.6	38.2	35.5
kodim09	45.6	37.9	34.4	kodim21	45.8	37.7	35.8
kodim10	47.0	39.0	36.5	kodim22	44.0	35.8	32.9
kodim11	44.6	36.7	34.1	kodim23	44.9	35.8	32.3
kodim12	46.4	38.6	35.4	kodim24	45.9	38.8	36.9
				Mean	45.0	37.3	34.7

Table 5. PSNR measure of image reconstruction quality of the proposed CFA with linear demosaicking, and the Bayer CFA with state-of-art nonlinear AHD¹⁸ and POCS²⁴ demosaicking.

reconstruction error and neither drowns out the other. This increases MSE by 1.97, 4.21 and 5.00 for the proposed CFA, AHD and POCS respectively, thereby demonstrating the robustness of the proposed CFA design to noise. The resulting images and their error from the original are shown in figure 5.

9. CHROMINANCE BANDWIDTH OF COMPETING CFA DESIGNS

In this section we analyze the chrominance bandwidths of the popular Bayer CFA as well as modern CFA designs by.^{4,7} We study the Bayer CFA with adaptive nonlinear frequency domain demosaicking that is representative of the state of the art. For the modern CFA designs by,^{4,7} we use the linear demodulate and filter demosaicking since that is one of their selling points. However, adaptive demosaicking algorithms can also be analyzed with ease.

Hirakawa & Wolfe⁴ present 4 CFA designs labeled A, B, C, D. All their CFAs use 2 carriers to modulate the two chrominance signals and their bandwidth is determined by computing half the euclidean “distance” between their carriers in the frequency domain. For patterns A, B this figure is $\frac{\pi}{4}$, for pattern C it is $\frac{\pi}{3\sqrt{2}}$ and for pattern D, it is $\frac{\pi}{3}$. This works out to 0.25, 0.24, 0.33, respectively, times the Nyquist frequency.

Finally, Condat’s⁷ pattern can be analyzed to have a chrominance bandwidth of $\frac{\pi}{3}$ which is 0.33 times the Nyquist frequency.

9.1 Chrominance Bandwidth of the Bayer CFA with Adaptive Demosaicking

THEOREM 2. *A demosaicking algorithm that extracts chrominance from a Bayer mosaiced image by demodulation and filtering has a chrominance bandwidth of no more than $\frac{\pi}{2}$.*

Proof. Consider a image patch containing a vertical edge. There are 2 copies of the R-B chrominance signal. If the chrominance bandwidth is set to greater than $\frac{\pi}{2}$, the copy at $(0, \pi)$ interferes with the luminance while the one at $(\pi, 0)$ interferes with the chrominance at (π, π) leaving no clean copy. \square

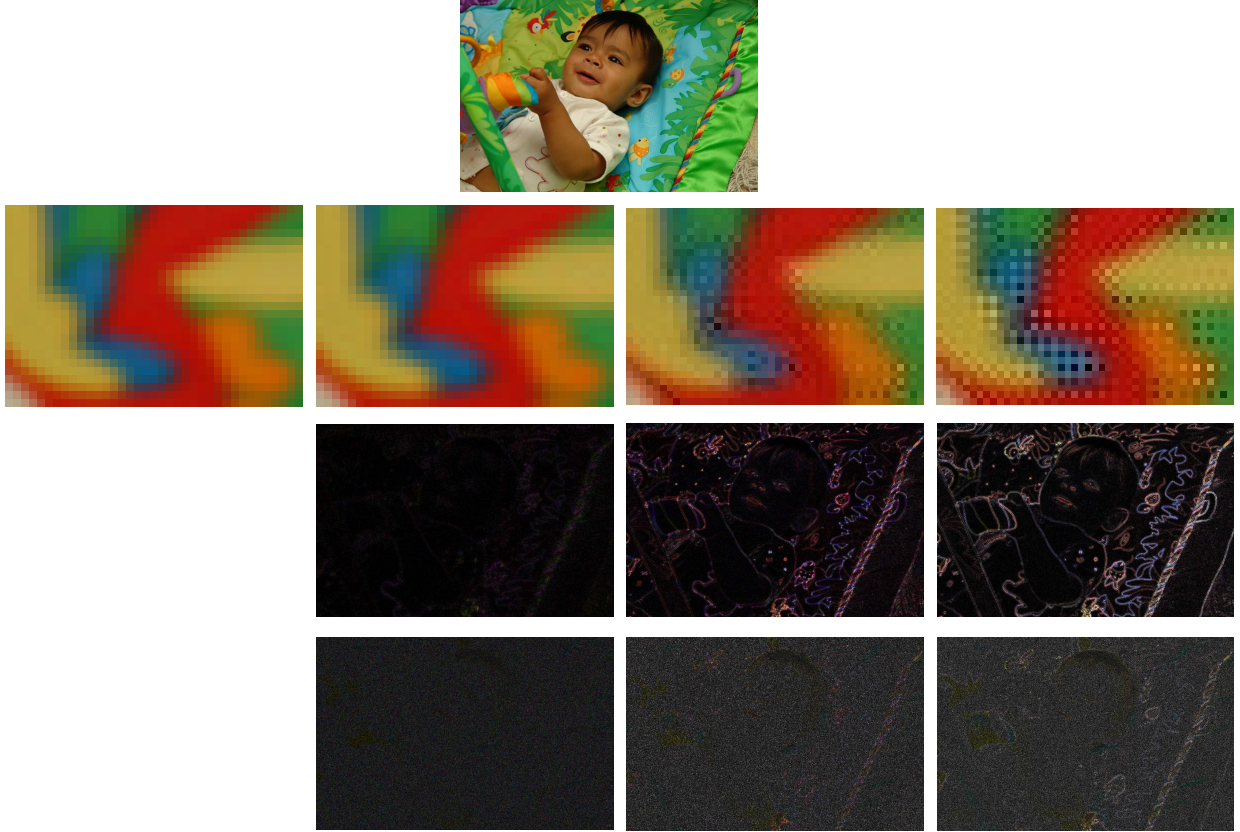


Figure 5. High resolution image. Top row: Original image. Second row: a small patch of the original image and as it's captured by the proposed CFA, Bayer AHD, Bayer POCS respectively. Third row: respective errors amplified by a factor of 10. Bottom row: respective errors amplified by a factor of 4 after addition of noise.

The optimum $r = 0.5$ design of section 8 has chrominance bandwidth of $\frac{\pi}{2}$ along the direction with coarser photosite pitch. This works out to 0.42 times the Nyquist frequency of the equivalent square photosite sensor with the same photosite area. This is substantially better than all recent CFA designs,⁴⁷ but marginally lower than the *theoretical upper bound* of 0.5 for the Bayer with adaptive demodulate and filter demosaicking.

10. CONCLUSION

In this paper we studied the problem of packing luminance and chrominance spectra using panchromatic CFAs with rectangular pixels. We introduced Chrominance Bandwidth Ratio, r , as a measure of image quality that roughly captures both chrominance bandwidth and crosstalk. We also introduced photosite aspect ratio as an important CFA design parameter. Using r as a design constraint we derived a CFA with a provably minimum number of pixels per unit sensor area that can faithfully capture the incident optical image.

The combination of Chrominance Bandwidth Ratio and photosite aspect ratio allowed us to design two interesting panchromatic CFAs, one provably outperforms the venerable color stripe CFA and the other outperforms the Bayer CFA in practice.

We also introduced a more realistic experimental setup than is common in academic work. This setup modeled the optical pipeline by starting with a high resolution input image and then simulated the effects of the OLPF, box filtering due to the non-zero size of photosites and aliasing due to high frequency leakage. After CFA filtering and demosaicking the image, it sharpened the output image as commercial systems usually do. Results of this rigorous test showed that our CFA design with efficient linear demosaicking outperforms the Bayer CFA with state of the art compute-intensive nonlinear demosaicking by a solid 7.6dB.

This paper raises the possibility of capturing much higher quality, artifact free images with comparable sensor complexity than is presently possible with the Bayer design. Furthermore, it shows that compute intensive non-linear demosaicking algorithms are not necessary to do so. Unlike other recent CFA designs, the proposed design does not sacrifice chrominance bandwidth to achieve these gains.

11. ACKNOWLEDGEMENTS

We would like to thank Keigo Hirakawa and Patrick Wolfe for providing us with a copy of their CFA design code.

REFERENCES

- [1] Panavision, “Panavision Genesis Digital Camera,” <http://www.panavision.com/publish/2007/11/09/Genesis.pdf>, 2 (2007).
- [2] Bayer, B., “Color imaging array,” (July 20 1976). US Patent 3,971,065.
- [3] Hirakawa, K. and Wolfe, P., “Spatio-spectral color filter array design for enhanced image fidelity,” in [*Proc. of IEEE ICIP*], II: 81–84 (2007).
- [4] Hirakawa, K. and Wolfe, P., “Spatio-Spectral Color Filter Array Design for Optimal Image Recovery,” *IEEE Transactions on Image Processing* **17**(10), 1876–1890 (2008).
- [5] Hirakawa, K. and Wolfe, P., “Second-generation color filter array and demosaicking designs,” in [*Proceedings of SPIE*], **6822**, 68221P (2008).
- [6] Hirakawa, K. and Wolfe, P., “Spatio-Spectral Sampling and Color Filter Array Design,” *Single-Sensor Imaging: Methods and Applications for Digital Cameras*, 137 (2008).
- [7] Condat, L., “A New Class of Color Filter Arrays with Optimal Sensing Properties,”
- [8] Li, Y., Hao, P., and Lin, Z., “Color Filter Arrays: A Design Methodology,” tech. rep., Technical Report, Department of Computer science, Queen Mary, University of London, 2008.
- [9] Alleysson, D., Susstrunk, S., and Héroult, J., “Color demosaicing by estimating luminance and opponent chromatic signals in the Fourier domain,” in [*Proc. IS&T/SID 10th Color Imaging Conf*], 331–336 (2002).
- [10] Alleysson, D., Susstrunk, S., and Héroult, J., “Linear demosaicing inspired by the human visual system,” *IEEE Transactions on Image Processing* **14**(4), 439–449 (2005).
- [11] de Lavarene, B., Alleysson, D., Durette, B., and Héroult, J., “Efficient demosaicing through recursive filtering,” in [*IEEE International Conference on Image Processing, 2007. ICIP 2007*], **2** (2007).
- [12] Dubois, E., “Frequency-domain methods for demosaicking of bayer-sampled color images,” *IEEE Signal Processing Letters* **12**(12), 847–850 (2005).
- [13] Dubois, E., “Filter design for adaptive frequency-domain Bayer demosaicking,” in [*Proceedings of the IEEE International Conference on Image Processing*], 2705–2708 (2006).
- [14] Lian, N., Chang, L., and Tan, Y., “Improved color filter array demosaicking by accurate luminance estimation,” in [*IEEE International Conference on Image Processing, 2005. ICIP 2005*], **1** (2005).
- [15] Hel-Or, Y., “The canonical correlations of color images and their use for demosaicing,”
- [16] Kimmel, R., “Demosaicing: Image reconstruction from color ccd samples,” *IEEE Trans. Image Processing* **8**, 1221–1228 (1999).
- [17] Chang, E., Cheung, S., and Pan, D., “Color filter array recovery using a threshold-based variable number of gradients,” in [*Proceedings of SPIE*], **3650**, 36 (1999).
- [18] Hirakawa, K. and Parks, T., “Adaptive homogeneity-directed demosaicing algorithm,” *IEEE Transactions on Image Processing* **14**(3), 360–369 (2005).
- [19] Ramanath, R., Snyder, W. E., Bilbro, G. L., and Sander, W. A., “Demosaicking methods for bayer color arrays,” *Journal of Electronic Imaging* **11**, 306–315 (2002).
- [20] Ramanath, R. and Snyder, W., “Adaptive demosaicking,” *Journal of Electronic Imaging* **12**, 633–642 (2003).
- [21] Zhang, L., Wu, X., and Member, S., “Color demosaicking via directional linear minimum mean square-error estimation,” *IEEE Transactions on Image Processing* **14**, 2167–2178 (2005).
- [22] Muresan, D. D. and Parks, T. W., “Demosaicing using optimal recovery,” *IEEE Transactions on Image Processing* **14**, 267–278 (2005).

- [23] Wu, X. and Zhang, N., “Primary-consistent soft-decision color demosaicking for digital cameras (patent pending),” *IEEE Transactions on Image Processing* **13**(9), 1263–1274 (2004).
- [24] Gunturk, B. K., Member, S., Altunbasak, Y., Member, S., and Mersereau, R. M., “Color plane interpolation using alternating projections,” *IEEE Trans. Image Processing* **11**, 997–1013 (2002).